Engineering and Technology Journal
Journal homepage: https://etj.uotechnology.edu.iq

Design and control of wireless charging system for electric vehicle

Basma A. Abbas*, Hosham S. Anead, Khalid F. Sultan

Electromechanical Engineering Dept., University of Technology-Iraq, Alsina'a street, 10066 Baghdad, Iraq.
*Corresponding author Email: basma.a.abass@uotechnology.edu.iq

HIGHLIGHTS

- Wireless charging for electric vehicles enables cable-free charging, enhancing convenience for drivers
- Recent advancements have significantly improved this technology, simplifying the charging process
- Enhancement of wireless charging efficiency for faster and more driver-friendly performance
- DC-DC boost converter raised the transferred voltage to 800 V within 20 KHz to reduce the wave signal ripple.
- The system's ability to charge the battery to 100% in just 900 seconds is a major advantage for wireless charging.

Keywords:
Wireless charging; EVs; Neural networks; IPT; Battery charge.

ABSTRACT

This study concentrated on utilizing a neural network controller and inductive power transfer to enhance the electric vehicle charging. Electric vehicles are a key transportation system component since they lower fuel costs, noise levels, and carbon emissions. The charging duration and operational battery efficiency are the primary obstacles to wireless charging in electric vehicles. In the beginning, the system was designed. It included the primary side (grid, rectifier, DC-DC boost converter, and DC-AC high-frequency inverter), mutual inductance (one coil transmitter and six coils receiver), and secondary side (single-phase rectifier and battery pack). A neural network controller has been employed to control the current and voltage to get fast charging. The simulation design and control have been simulated using MATLAB 2022b. As a result, the DC-DC boost converter raised the transferred voltage to 800 V within 20 KHz to reduce the wave signal ripple. In comparison, a neural network controller kept the transfer voltage and constant current to 800 V and 100 A during charging from 10% to 100%. Moreover, a neural network controller worked on charging the system within 15 minutes as a fast-charging technique. Also, the behavior and value of the voltage transmitted to the battery have been verified.

1. Introduction

Electric vehicles (EVs) have risen rapidly due to decreasing dioxide emissions, and power source electricity is much less expensive than gasoline. As a result, there is a need for continuous enhancements to charging infrastructure, particularly wireless infrastructure, which must work with both public and residential charging stations and be made for private, business, and public uses [1,2]. Wireless power transmission technology can do away with cables, making electronic gadgets more portable, convenient, and safe for all users than cable connections. Therefore, the availability of wireless charging stations addresses the issues of charger connectivity, charging time, and range anxiety—possibly the largest barriers to the broad use of EVs [3]. Capacitive Wireless Charging System (CWCS), Permanent Magnetic Gear Wireless Charging System (PMWC), Inductive Wireless Charging System (IWCS), and Resonant Inductive Wireless Charging System (RIWC) are the four wireless power transmission (WPT) technologies. Several techniques exist for WPT, with the capacitive and inductive approaches having the most practical applications. IPT and RIWC are the most used techniques for working with various power outputs and gap sizes. Moreover, IPT may be utilized for large air gaps of several meters and has a substantially larger output power than CPT. At the same time, CPT is only appropriate for power transfer with naturally narrow gap distances because of limitations on the generated voltage and is only suitable for low-power applications with extremely tiny air gaps between 10 to 4 m [4]. On the other hand, Microwaves may transmit power over great distances and with high output power using frequencies between 1 GHz and 1000 GHz. This technology is expensive and harmful to humans [5,6].

Compensation circuits, including an inductor and a capacitor, should be considered when applying WPT using IPT. There are four categories of basic compensation topologies: Series-Series (SS), Series-Parallel (SP), Parallel-Parallel (PP), and Parallel-Series (PS) [7,8]. Regarding power transfer efficiency and maximum output power, SS- topology proved to be better than SP-topology, which maintains high efficiency throughout the WPT process but depends on variations in resonance frequency and coupling coefficient [9]. Many researchers have concentrated on battery conservation strategies based on the principles of

http://doi.org/10.30684/etj.2025.155228.1872
Received 29 December 2024; Received in revised form 12 February 2025; Accepted 13 February 2025; Available online 10 March 2025
2412-0758/University of Technology-Iraq, Baghdad, Iraq

constant voltage or constant current by employing control theories, such as proportional-integral (PI), fuzzy logic, and adaptive neuro-fuzzy (ANFIS) controllers. These theories can control the voltage of the primary side or the voltage and current of the secondary side. It was the most effective because it simultaneously used nonlinear control theories to control voltage and current [10-13]. Finally, the power transfer procedure achieved roughly 6.6 KW to 50 KW in 30 minutes by connecting compensatory circuits (SS and SP) utilizing the IWCS and RIWC techniques. Researchers are still interested in finding ways to improve the efficiency of charging batteries faster by increasing the transferred power [14-17]. In this research, a current and voltage strategy were controlled together via the neural network. The artificial neural networks (ANN) controller determines the number of secondary coils to get a higher transferred power depending on the S-S connection topology that was not used before. This study presents the fundamental idea of the wireless charging system, the charging of electric vehicles, and a mathematical model. Section II focuses on the equation and equivalent circuit model.

2. Wireless charging

This section deals with the wireless power transmission work principle and presents the mathematical equation for wireless power transmission.

2.1 Wireless charging system for electric vehicle charging

The wireless charging system states that several elements, including air gaps, size, form, and material, should be considered to improve the power transfer. How to charge an electric vehicle's battery from the grid is explained in Figure 1. The charging procedure from grid to battery return can be broken down into four steps: using a rectifier to convert the voltage from AC to DC, using an inverter to convert the DC to AC with high frequency, using mutual inductance to transfer the power, and using a rectifier to convert the voltage from AC to DC [18,19].

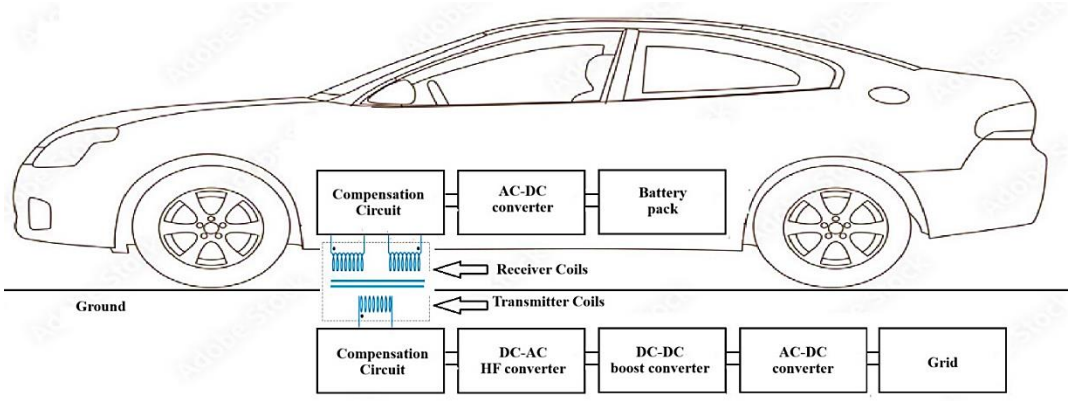

Figure 1: Wireless power transfer system for electric vehicle

2.2 Mathematical model of wireless power transfer (WPT)

The four compensation topologies, series-series (S-S), Parallel-Parallel (P-P), Parallel-Series (P-S), and Series-Parallel (S-P), are the most common compensation types utilized in the sending and receiving circuits of the wireless power transmission system. The equivalent circuit model from WPT is based on the locations of the compensatory capacitor for the coil [20, 21]. Figure 2 shows the equivalent circuit for the WPT system, which contains one transmitting coil while the receiver side continues with multiple coils.

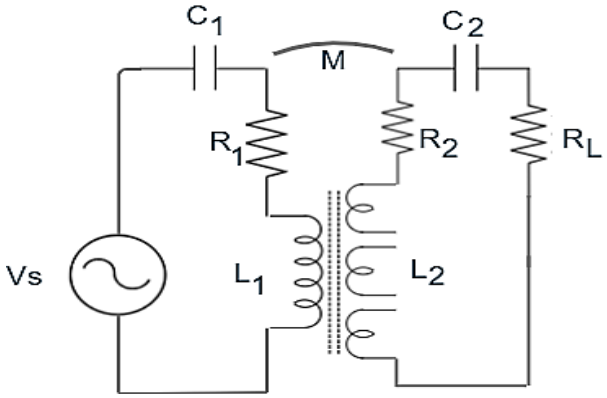

Figure 2: Simplified circuit model of the WPT system

The given circuit is represented mathematically using Kirchhoff's voltage law. The following is an expression for the voltage that passes through the transmitting coil [7]:

$$V_s = \left(R_1 + j\omega_0 L_1 + \frac{1}{j\omega_0 c_1}\right) I_1 + j\omega_0 M I_2 \quad (1)$$

Where the supply voltage is V_s, mutual inductance is M, primary and secondary currents are I_1 and I_2 respectively, angular frequency is ω0, and primary resistance, inductance, and capacitance are R_1, $L_1$and c_1 respectively. When Kirchhoff's law is applied to the circuit's receiver side, it produces:

$$0 = \left(R_2 + j\omega_0 L_2 + \frac{1}{j\omega_0 c_2}\right) I_2 + j\omega_0 M I_1 \quad (2)$$

Where the secondary resistance, inductance, and capacitance are denoted by R_2, L_2 and c_2 respectively. A matrix below can be used to express Equations (1) and (2):

$$\begin{bmatrix} Z_1 & Z_m \\ Z_m & Z_2 + Z_L \end{bmatrix} \begin{bmatrix} I_1 \\ I_2 \end{bmatrix} = \begin{bmatrix} V_s \\ 0 \end{bmatrix} \quad (3)$$

The parameters of the mutual impedance (Z_m) load impedance (Z_L), primary coil impedance (Z_1), and secondary coil (Z2) are represented according to Equations (4- 7), respectively.

$$Z_1 = \left(R_1 + j\omega_0 L_1 + \frac{1}{j\omega_0 c_1}\right) \quad (4)$$

$$Z_2 = \left(R_2 + j\omega_0 L_2 + \frac{1}{j\omega_0 c_2}\right) \quad (5)$$

$$Z_m = (j\omega_0 M) \quad (6)$$

The primary and secondary currents can be estimated by resolving Equation (3) to be:

$$Z_L = (R_L) \quad (7)$$

$$I_1 = \frac{V_s(Z_2+Z_L)}{Z_1(Z_2+Z_L)-Z_m^2} \quad (8)$$

$$I_2 = \frac{V_s Z_m}{Z_1(Z_2+Z_L)-Z_m^2} \quad (9)$$

The induced voltage from the primary to the secondary coils can be found by:

$$V_{12} = Z_m I_2 \quad (10)$$

The value of the reflected impedance (Z_r) depends on three parameters: load impedance, capacitance, and receiver impedance, which come from dividing the transmitter-dependent voltage by the transmitter current, as shown in Equation (11).

$$Z_r = V_{12}/I_1 = Z_m^2/(Z_2+Z_L) \quad (11)$$

While the relationship between the primary and reflected impedances to find input impedance (Z_{in}) as shown in Equation (12).

$$Z_{in} = Z_1/Z_m^2/(Z_2+Z_L) \quad (12)$$

Finally, Equations (13) and (14) are used to calculate the transmitted power (P_t) and output power (P_L) [7]:

$$P_L = Re(Z_L^*)|I_2|^2/2 \quad (13)$$

$$P_t = Re(Z_m^*)|I_1|^2/2 \quad (14)$$

3. System methodology design

This section deals with coil design and methodology of artificial neural networks

3.1 Coil parameters

This study tested the effectiveness of a dynamic WPT system for EV charging that uses a converter and a controller. The WPT system still works, consisting of 19 transmitter coils and one receiver coil. The coil in this research was designed based on a previous study, and the parameters of this coil are 20 turns, 70 mm inner radius, 3 mm wire radius, 2 mm air gap between turns, and 170 mm outer radius. Each coil is circular and the same size [7].

3.2 Neural network controller

The process of data processing in the human brain is similar to that of artificial neural networks (ANN), considered one of the computational methods. Interconnected nodes (also known as "neurons") are arranged in input, hidden, and output layers,

which form the main structure of ANNs. When the network gains knowledge from data, the weight assigned to each connection between nodes changes. ANNs are employed for several applications, such as pattern recognition, the healthcare industry for X-ray detection, and armed attack analysis [22]. Figure 3 shows a block diagram of an ANN algorithm structure.

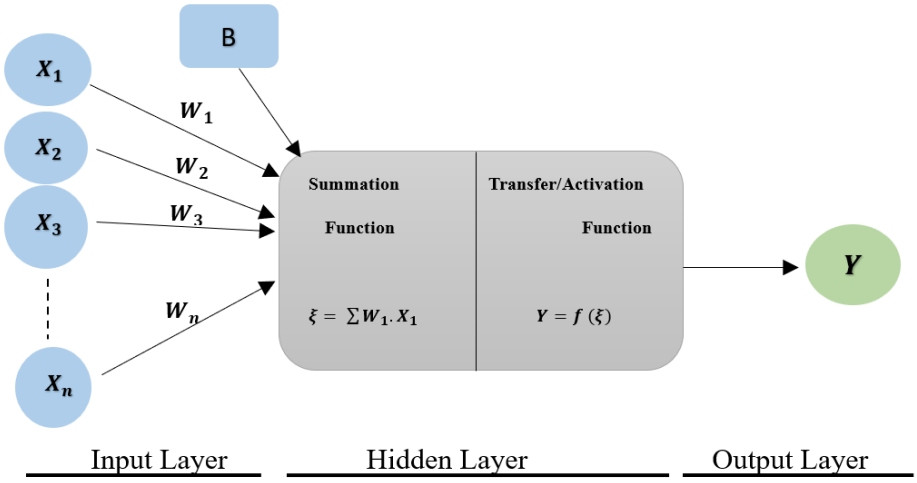

Figure 3: Structure of the ANN algorithm construction [22]

According to prior research [23], ANN control performance was one of the optimal methods for controlling dynamic systems in different fields. It can be represented as a mathematical equation, as shown in equation 15, for each input layer, hidden layer, and output layer.

$$y = x_1 w_1 + x_2 w_2 + \cdots + x_n w_n + b \quad (15)$$

where, x represents the input data, y represents the output data, b represents the bias and w represents the weight.

4. Results and discussion

The EVs were designed with both a primary and secondary side. A three-phase voltage source (380 volts and 50 Hz), an AC-DC converter, and a DC-DC boost converter type diode comprise the first part to generate high voltages. The electricity is converted to DC-AC high frequency using an inverter-type insulated-gate bipolar transistor (IGBT). A lithium-ion battery, an AC-DC rectifier, and mutual inductance (six coils) make up the receiving part, as shown in Figure 4. The simulation design has been implemented using MATLAB 2022b. Table 1 also shows the characteristics of the simulation model for the EV wireless charging system based on the electrical circuit components.

Table 1: The characteristics of the EV system

Parameters	**Value**
Input voltage	380 V
L for ac-dc converters	200mH
C for ac-dc converters	5000µF
Switching frequency	20KHz
L for dc-cd boost converter	250µH
C for dc-cd boost converter	0.0005F
Switching frequency for DC-AC converter	20KHz
L filter	2mH
Mutual inductance	
R_m	0.005Ω
L_m	85.4 µH
Battery Parameters	
Type of Battery	Lithium-Ion
Nominal voltage	800 v
Initial state-of-charge (%)	50 %

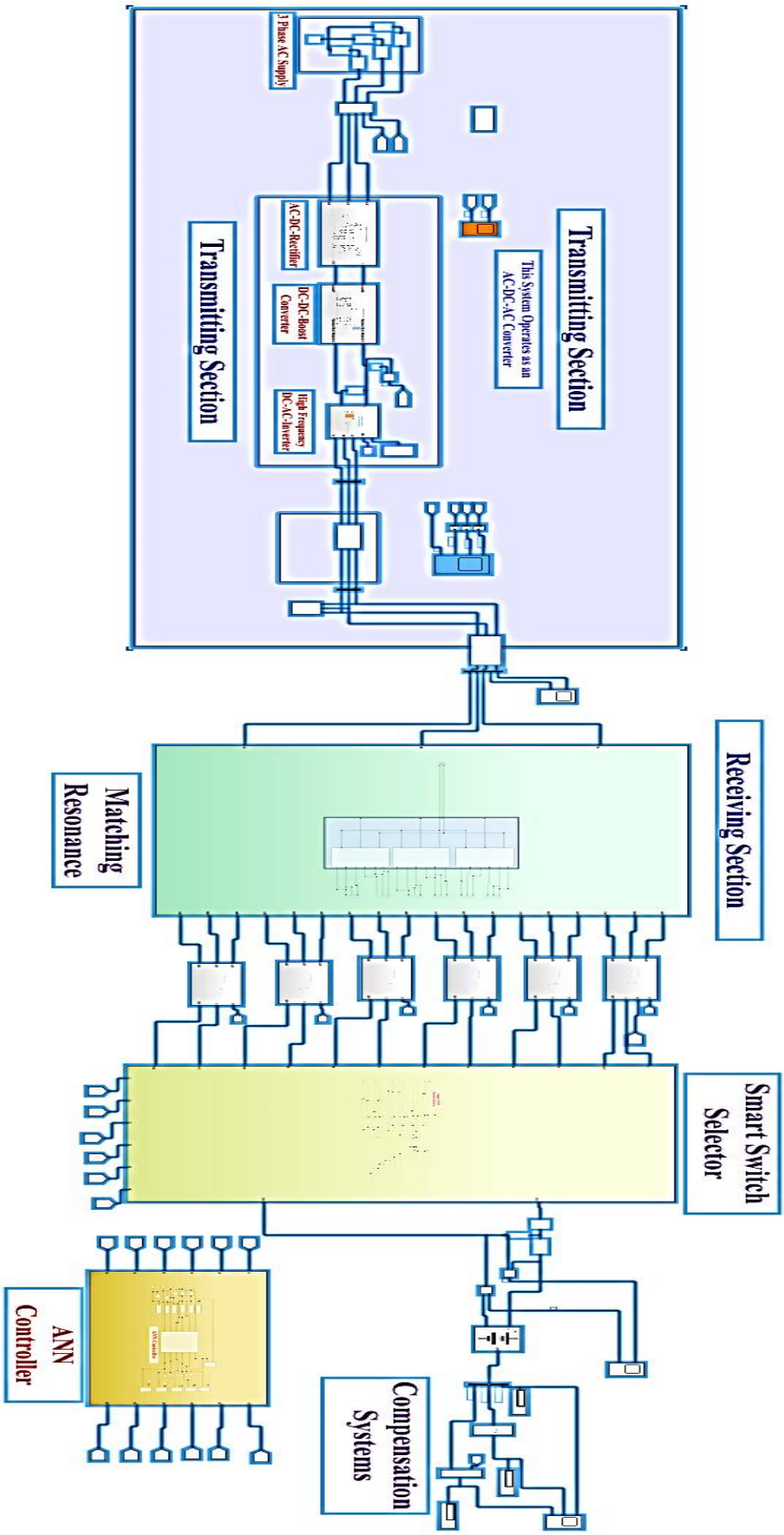

Figure 4: MATLAB simulation model for wireless charging of EV with ANN

This research employed a constant current-constant voltage (CC-CV) control method with an artificial neural network controller (ANNC) to maintain a constant current and voltage throughout a certain charging stage. This design improved the system's efficiency and battery life. The technique was improved by connecting numerous coils in parallel with the primary receiving coil, which is triggered based on the battery's charging requirements. This procedure is managed by an intelligent selection circuit driven by the intelligent neural network, which optimizes the charging path based on the battery's state and charging needs. The feed-forward neural network was utilized, which has three layers: one input, one hidden, and one output. Fifteen thousand data points were divided into three categories: 9,000 for training, 3,000 for validation, and 3,000 for testing. Figure 5 (a) represents the error curves with the number of epochs (the number of iterations in which the neural network weights were updated during training) resulting from training a neural network model, where the blue curve represents the error on the training data, the green curve represents the error on the validation data and the red curve represents the error on the test data. In contrast, the green circle indicates where the model achieved the best performance on the validation data and represents the lowest validation error. The diagram is displayed using a logarithmic scale, which helps display the large error-value changes. At first, the error appeared very high for all data (training, validation, test), which was normal because the model had not been learned yet. As the training progresses (increasing the number of epochs), the error on the training data decreases significantly as the model improves its representation of the data. It is noticeable that the validation error follows the same pattern but becomes stable at a certain point, where at epoch 222, the model achieves the lowest validation error (0.052456), indicating that this is the optimal model before any possibility of increasing complexity or overfitting occurs, while the red line (test) shows the performance of the final model after training which seems close to the validation performance. The results show that the best performance is achieved at epoch 222. In comparison, the curves show that the model is well optimized without overfitting, as there is no significant increase in validation error after the optimal epoch. In conclusion, the neural network performed best at epoch 222, balancing training accuracy and validation generalization ability. This indicates that the model is well-optimized and can effectively predict new data within the given limits. Figure 5 (b) shows the relationship between the outputs of the neural network model and the actual targets for the training, validation, and testing stages, as well as all the data together. Each graph represents a relationship between the neural network's target and predicted values (Output).

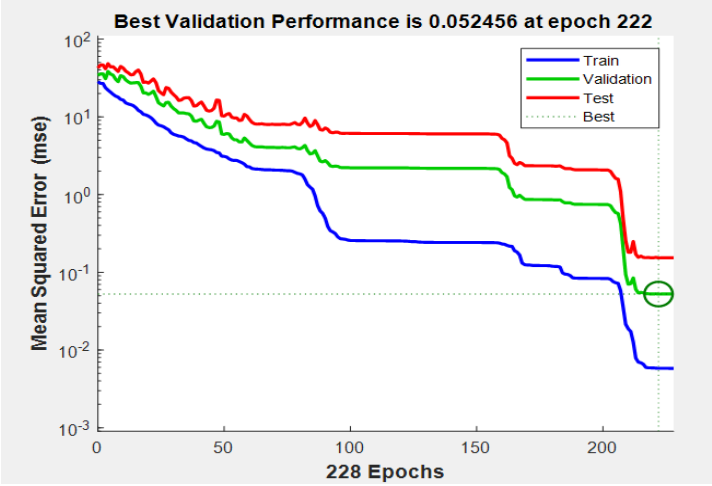

(a)

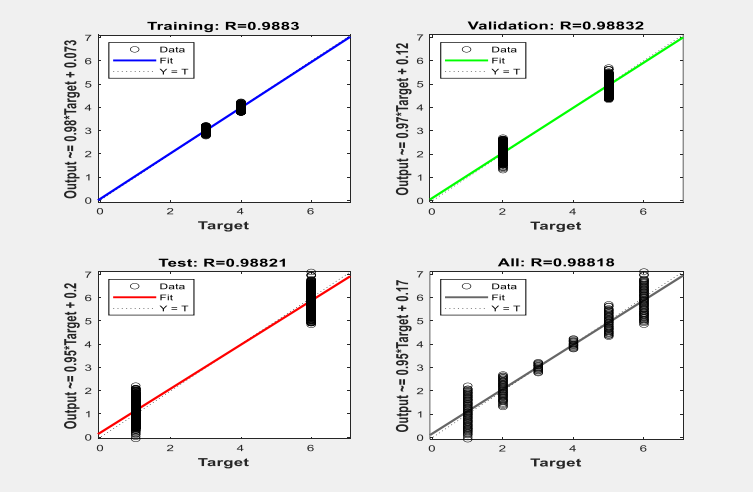

(b)

Figure 5: The ANN training performance matrices are (a) mean square error (MSE) performance measure and (b) regression (ROC) measure

The Y = T lines (dashed line) represent the ideal relationship between the outputs and the target values, where the predicted values should equal the actual values. In Training, the blue graph shows the neural network's performance on the training data, and the correlation coefficient (R) at this stage is equal to 0.9883, indicating a high agreement between the outputs and the target values. In contrast, the green graph in Validation shows the network's performance on the validation data. The correlation coefficient (R) equals 0.98832, indicating the model has good generalization ability. In the test (test), the red graph shows the neural network's performance on the test data. The correlation coefficient (R) is equal to 0.98821, reflecting the consistent performance of the model on new data. Finally, the black graph (all data) shows the combined training, validation, and test data. At the same time, the correlation coefficient (R) equals 0.98818, indicating that the model shows strong and consistent performance across all data. The correlation coefficient (R) was very close to the ideal value (1), indicating that the outputs generated by the model are highly consistent with the real targets. The points close to the Y = T line show that the errors are few, indicating that the neural network was able to learn well and achieve predictions with high accuracy. The results showed that the model trained using the neural network performed excellently across the training and validation stages. For the test, the high correlation coefficient and the distribution of points close to the ideal line indicate that the model has good generalization ability and high accuracy in predicting target values.

Figure 6 shows the relationship between the voltage measured in volts (V) and time in seconds (sec), where the charging process is controlled using a neural network controller to ensure that the voltage is maintained at a value close to 800 volts. At the beginning of charging, we notice a rapid increase in the voltage from a value close to 785 volts to about 800 volts during the first 100 seconds. This behavior indicates the first stage of charging, fast charging, in which the neural network controller operates the largest number of coils to achieve rapid stability. At this stage, the current flow is high to facilitate fast battery charging. After the voltage rises quickly at the beginning, the charging process begins to slow down gradually, where we notice a slight increase in the voltage after 100 seconds until the end of the period (900 seconds). This slow change indicates that the neural network controller adapts to the dynamic system (battery dynamics) to ensure that charging continues with high efficiency and prevents any fluctuations or sudden drops in voltage. Next, we notice that the voltage increases slowly and almost linearly from 800V to about 805V at the end of the graph. This behavior indicates that the battery is approaching full charge (State of Charge), where the neural network controller precisely controls the voltage to maintain the stability of the charging process and prevent exceeding the safe limits of the battery. The results from the graph show that the neural network controller succeeded in maintaining the voltage value very close to 800V throughout the charging period, as it worked very efficiently to maintain a balance between charging speed and battery protection, which is ideal for use in electric vehicles.

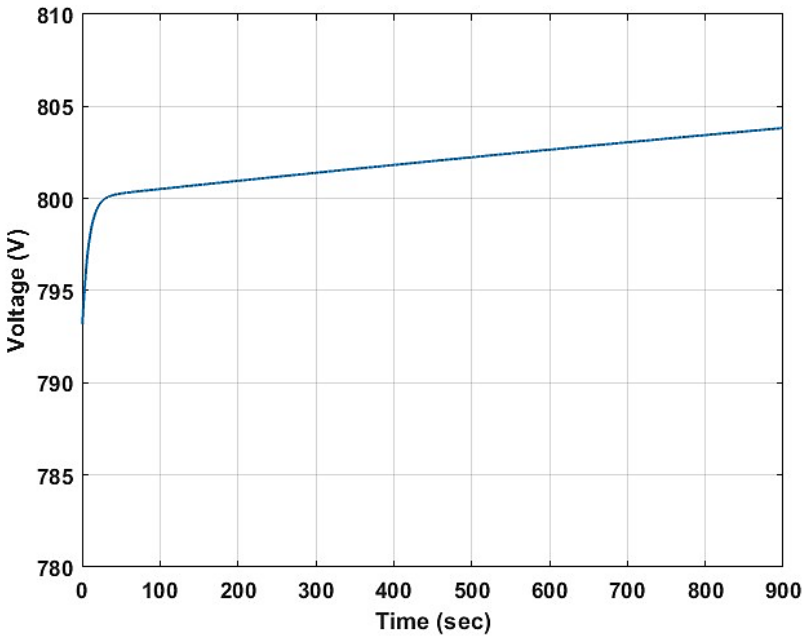

Figure 6: Battery voltage

Figure 7 shows the relationship curve between the electric current and time during the wireless charging process of an electric vehicle using the ANNC. At the beginning of the charging process, the current rises rapidly from 0 amperes to about 40 amperes, indicating an immediate response of the system to deliver energy to the battery. This part reflects the dynamic performance of the ANNC, which begins to adjust the current quickly. In the second stage, which starts from 100 to 600 seconds, the current gradually increases from 40 amperes until it reaches 90 amperes. The increase is smooth and free of significant fluctuations, indicating that the neural network controller continuously monitors the current and adjusts it based on the battery's condition to ensure safe charging. When the time approaches 900 seconds, the current reaches the target value of 100 amperes and stabilizes. This indicates the efficiency of the ANNC in maintaining the required current with high accuracy and ensuring the effective continuation of charging. Here, the role of the neural network controller appears as it works to improve the performance of the charging process by continuously adapting to system changes (such as battery conditions and energy needs). It is characterized by its ability to stabilize the electric current at the required value (100 amperes) without exceeding it or causing fluctuations that

lead to instability of charging. On the other hand, the ability to adjust the current in this way means that the system can avoid overcharging or technical problems such as overheating. Also, the stable current of 100 amps achieves an ideal charging speed without stressing the battery, which increases the efficiency of the charging process and extends the battery life. The results showed that the performance of the ANNC in controlling the wireless charging process is characterized by its ability to gradually reach the target current (100 amps) and maintain the current at the required value steadily and stably, in addition to ensuring the efficiency and safety of charging without fluctuations or excesses.

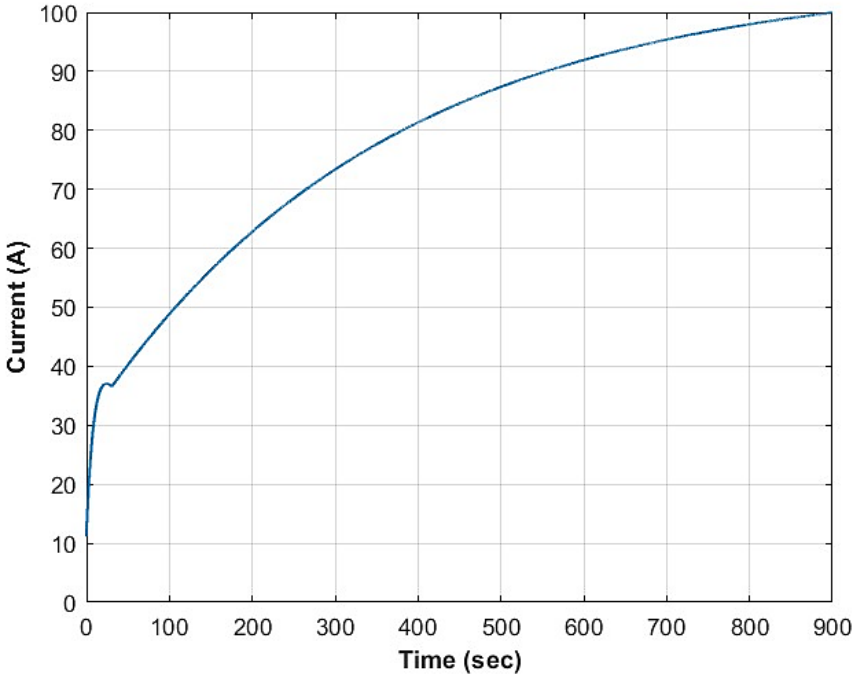

Figure 7: Battery current

Figure 8 shows the electric battery's state of charge (SOC) during the wireless charging. The charging process was controlled using ANNC, which controlled the number of secondary coils (six coils connected in parallel) to achieve charging the 100 Ah battery as quickly as possible within 900 seconds. The SOC starts at approximately 10% and increases rapidly in the first 200 seconds. At this stage, power is transferred very efficiently through the secondary coils with the help of the precise coordination of the ANNC. After that, the charging rate gradually decreases, reaching about 80%. This slowdown is normal and occurs due to the characteristics of batteries, where the efficiency of receiving energy decreases as the battery approaches its maximum state. After that, the charging percentage gradually approaches 100%, stabilizing the curve. Here, the role of the ANNC appears in controlling the number of activated secondary coils based on the battery state, which ensures maximum energy transfer efficiency.

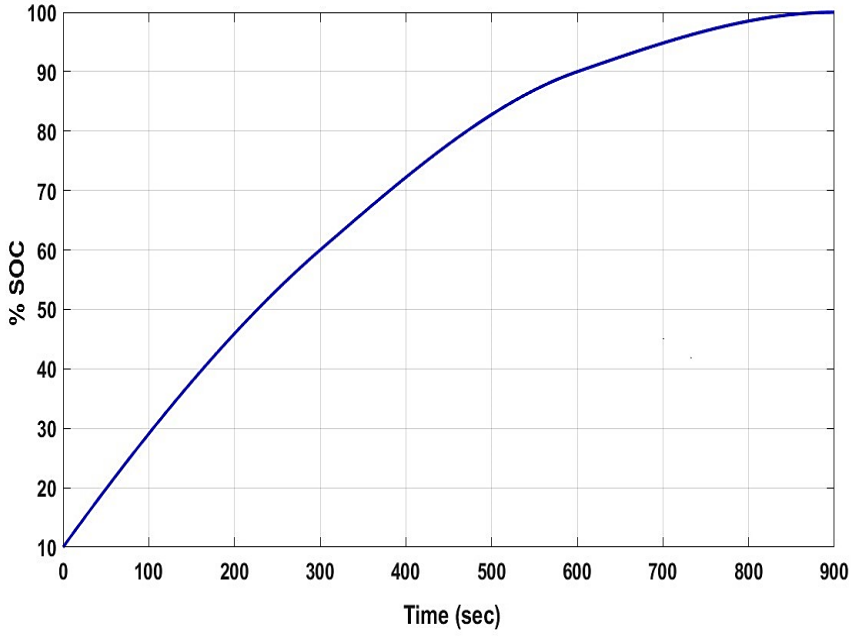

Figure 8: State of charge battery

On the other hand, the current and voltage were adjusted to charge the battery smoothly without excessive stress or the risk of overheating. By contributing to the intelligent control of the coils and the perfect balance of energy, the battery was fully charged in a record time of 900 seconds. The system's ability to charge the battery to 100% in a very short time of 900 seconds is a great advantage for wireless charging systems. It is noted that there were no sharp fluctuations or oscillations, indicating the efficiency of the system and the stability of the charging process.

This research was verified with other research that indicated the current range of fast charging is between 100-400A, whereas in this study, the current value was 100 A [24]. On the other hand, the behavior and value of the voltage supplied to the battery (800 V) in this research were verified with the behavior of the voltage in the study, where the researcher used fuzzy and ANFIC controllers to control the current only as shown in Figure 9 [12].

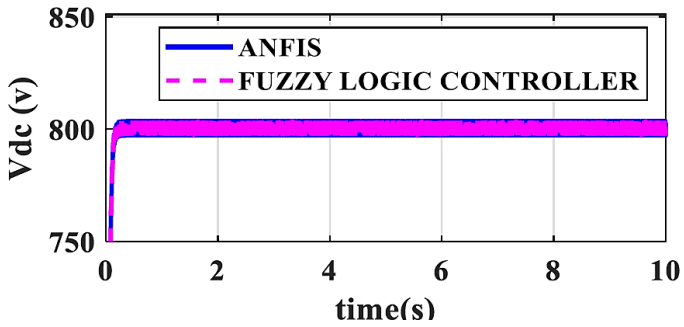

Figure 9: Voltage DC

5. Conclusion

Inductive power transfer technology with an intelligent controller has been proposed in this paper. The neural network controller maintained a voltage value close to 800 V throughout the charging period. It worked very efficiently to maintain a balance between charging speed and battery protection. Also, the performance of the ANNC was characterized by its ability to gradually reach the current target (100 amps) and maintain the current at the required value steadily and stably, in addition to ensuring the efficiency and safety of charging without fluctuations or excesses. Finally, the system's ability to charge the battery up to 100 % in a very short time of 900 seconds was a great advantage for wireless charging systems. On the other hand, it was noted that there were no sharp fluctuations or oscillations in the efficiency of the system and the stability of the charging process.

Author contributions

Conceptualization and methodology, **B. Abbas**, **H. Anead** and **K. Sultan**.; formal analysis, **B. Abbas**, **H. Anead** and **K. Sultan**.; investigation and data curation, **B. Abbas**, **H. Anead** and **K. Sultan**.; validation, **B. Abbas**, **H. Anead** and **K. Sultan**.; visualization, **B. Abbas**, **H. Anead** and **K. Sultan**.; writing—original draft preparation, **B. Abbas**.; writing—review and editing, **B. Abbas**, **H. Anead** and **K. Sultan**.; supervision, **B. Abbas**, **H. Anead** and **K. Sultan**.; project administration: **B. Abbas**, **H. Anead** and **K. Sultan**.: all authors have read and agreed to the published version of the manuscript.

Funding

This research received no specific grant from any funding agency in the public, commercial, or not-for-profit sectors.

Data availability statement

The data that support the findings of this study are available on request from the corresponding author.

Conflicts of interest

The authors declare that there is no conflict of interest.

References

[1] G. Palani, U. Sengamalai, P. Vishnuram, B. Nastasi, Challenges and Barrier of Wireless Charging Technologies for Electric Vehicles, Energies, 16 (2023) 2138. https://doi.org/10.3390/en16052138

[2] Y. Yasa, A system efficiency improvement of DC fast-chargers in electric vehicle applications: Bypassing second-stage full-bridge DC-DC converter in high-voltage charging levels, Ain Shams Eng. J., 14 (2023) 102391. https://doi.org/10.1016/j.asej.2023.102391

[3] J. M. Miller, O. C. Onar, M. Chinthavali, Primary-Side Power Flow Control of Wireless Power Transfer for Electric Vehicle Charging, IEEE J. Emerging Sel. Top. Power Electron., 3 (2014) 147-162. https://doi.org/10.1109/JESTPE.2014.2382569

[4] B. Mohan, M.V. Ramesh, V.R. Rajan, D. Rene Dev, Designing of A Wireless Charging System for Electric Vehicles, J. Theor. Appl. Inf. Technol., 102 (2024) 426-439.

[5] B. Hu, Li. Hao, T. Li, H. Wang, Y. Zhou, X. Zhao, X. Hu, A Long-Distance High-Power Microwave Wireless Power Transmission System Based on Asymmetrical Resonant Magnetron and Cyclotron-Wave Rectifier, Energy Rep., 7 (2021) 1154-1161. https://doi.org/10.1016/j.egyr.2020.12.026

[6] A. Mahmood, A. Ismail, Z. Zaman, H. Fakhar, Z. Najam, M. S. Hasan, S. H. Ahmed, A Comparative Study of Wireless Power Transmission Techniques, J. Basic Appl. Sci. Sci. Res., 4 (2014) 321-326.

[7] M. Amjad, M. F. Azam, Q. Ni, M. Dong, E.A. Anasari, Wireless Charging Systems for Electric Vehicles, Renewable Sustainable Energy Rev., 167 (2022) 112730. http://dx.doi.org/10.1016/j.rser.2022.112730

[8] Z. Wang, Y. Shi, X. Ma, Y. Wei, A Coreless Hybrid Magnetic Coupling Coil Structure for Dynamic Wireless Power Charging System, 7th Int. Conf. Power and Energy Systems Engineering, Energy Rep., 6 (2020) 843-850. https://doi.org/10.1016/j.egyr.2020.11.123

[9] M. T. Nguyen, C. V. Nguyen, L. H. Truong, A. M. Le, T. V. Quyen, A. Masaracchia, and K. A. Teague, Electromagnetic Field based WPT Technologies for UAVs: A Comprehensive Survey, Electronics, 9 (2020) 461. https://doi.org/10.3390/electronics9030461

[10] A. Smagulova, M. Lu, A. Darabi, M. Bagheri, Simulation Analysis of PI and Fuzzy Controller for Dynamic Wireless Charging of Electric Vehicle, IEEE Int. Conf. Environment and Electrical Engineering and IEEE Industrial and Commercial Power Systems Europe (EEEIC / I&CPS Europe), Madrid, Spain, 1-6, 2020. https://doi.org/10.1109/EEEIC/ICPSEurope49358.2020.9160851

[11] P. R. Shabarish, R. P. Krishna, B. Prasanth, K. Deepa, P.V. Manitha, V. Sailaja, Fuzzy based Approach to Enhance the Wireless Charging System in Electric Vehicles, IEEE 4th Int. Conf. Electronics, Communication and Aerospace Technology (ICECA),176-181, 2020. https://doi.org/10.1109/ICECA49313.2020.9297505

[12] P. Rames, A. Yamini, M. S. Ram, V. Bhargavi, P. B. Sujith, N. Jyothis, A Novel ANFIS Controller-Based Grid Connected EV Charging System with Constant Current Control Topology, Int. J. Sci. Res. Comput. Sci. Eng. Inf. Technol., 9 (2023) 342–350. https://doi.org/10.32628/IJSRCSEIT

[13] H. Q. Hameeda, H. S. Aneada and K. F. Sultanb, ANFIS Control of Four-Quadrant DC/DC Chopper for Wireless EV Charging, Eng. Technol. J., 42 (2024) 1122- 1137. https://doi.org/10.30684/etj.2024.146136.1673

[14] V. B. Vu, V. T. Doan, V. L. Pham, W. Choi, A New Method to Implement The Constant Current-Constant Voltage Charge of The Inductive Power Transfer System for Electric Vehicle Applications, IEEE, ITEC Asia-Pacific, (2016) 449-453. https://doi.org/10.1109/ITEC-AP.2016.7512996

[15] M. A. Roslan, N. N. Nanda, S. Yusoff, Series-Series and Series-Parallel Compensation Topologies for Dynamic Wireless Charging, IIUM Eng. J., 22 (2021) 199-209. https://doi.org/10.31436/iiumej.v22i2.1660

[16] T. A. Shikdar, Sh. Dey, S. Mumtahina, M. M. Rashid, G. M. Chowdhury, Design and Simulation of Single Phase and Three Phase Wireless Power Transfer in Electric Vehicle Using MATLAB/Simulink, Int. Conf., Electrical and Electronics Engineering, Singapore, 83-104, 2022. https://doi.org/10.1007/978-981-19-1677-9_8

[17] S. Uk Jeon, J. W. Park, B. K. Kang, H. Jin Lee, Study on Battery Charging Strategy of Electric Vehicles Considering Battery Capacity, IEEE Access, 9 (2021) 89757-89767. https://doi.org/10.1109/ACCESS.2021.3090763

[18] P. R. Shabarish, R. P. Krishna, B. Prasanth, K. Deepa, P.V. Manitha, V. Sailaja, Fuzzy based approach to enhance the wireless charging system in electric vehicles, IEEE 4th Int. Conf. Electronics, Communication and Aerospace Technology (ICECA), (2020) 176-181. https://doi.org/10.1109/ICECA49313.2020.9297505

[19] Erhuvwu, A., Modeling of Magnetic Resonance Wireless Electric Vehicle Charging, Electronic Theses and Dissertations, Georgia Southern University, 2019.

[20] P. Cao1, Y. Lu, Ch. Lu, X. Wang, W. Xu, H. Zhang, A Study on Modeling of Wireless Charging System Based on Fuzzy Logic Control, Int. J. Phys.: Conf. Ser., 1983 (2021) 012053. https://doi.org/10.1088/1742-6596/1983/1/012053

[21] Y. H. Sohn, B. H. Choi, E. S. Lee, G. C. Lim, G.-H. Cho, C. T. Rim, General Unified Analyses of Two-Capacitor Inductive Power Transfer Systems: Equivalence of Current-Source SS and SP Compensations, IEEE Trans. Power Electron., 30 (2015) 6030-6045. https://doi.org/10.1109/TPEL.2015.2409734

[22] Aggarwal, C.C., Neural Networks and Deep learning, Cham: springer, 2018.

[23] Ch. Zhang, X. Xu, Y. Li, J. Huang, Ch. Li, W. Sun, Research on SOC Estimation Method for Lithium-Ion Batteries Based on Neural Network, World Electr. Veh. J., 14 (2023) 275. https://doi.org/10.3390/wevj14100275

[24] V. Sawant, P. Zambare, D. C. Fast Charging Stations for Electric Vehicles: A Review, Energy Convers. Econ., 5 (2024) 54-71. https://doi.org/10.1049/enc2.12111